

Article

Low-Temperature Diffusion of Au and Ag Nanolayers for Cu Bonding

Sangmin Lee , Sangwoo Park and Sarah Eunkyung Kim * 

Department of Semiconductor Engineering, Seoul National University of Science and Technology, Seoul 01811, Republic of Korea

* Correspondence: eunkyung@seoultech.ac.kr

Abstract: With the recent rapid development of IT technology, the demand for multifunctional semiconductor devices capable of high performance has increased rapidly, and the miniaturization of such devices has also faced limitations. To overcome these limitations, various studies have investigated three-dimensional packaging methods of stacking devices, and among them, hybrid bonding is being actively conducted during the bonding process. studies of hybrid bonding during the bonding process are active. In this study, Cu bonding using a nano passivation layer was carried out for Cu/SiO₂ hybrid bonding applications, with Au and Ag deposited on Cu at the nano level and used as a protective layer to prevent Cu oxidation and to achieve low-temperature Cu bonding. Au was deposited at about 12 nm, and Ag was deposited at about 15 nm, with Cu bonding carried out at 180 °C for 30 min, after which an annealing process was conducted at 200 °C for one hour. After bonding, the specimen was diced into a 1 cm × 1 cm chip, and the bonding interface was analyzed using SEM and TEM. Additionally, the 1 cm × 1 cm chip was diced into 2 mm × 2 mm specimens to measure the shear strength of the bonded chip, and the average shear strength of Au and Ag was found to be 5.4 and 6.6 MPa, respectively. The degree of diffusion between Au-Cu and Ag-Cu was then investigated; the diffusion activation energy when Au diffuses to Cu was 6369.52 J/mol, and the diffusion activation energy when Ag diffuses to Cu was 17,933.21 J/mol.

Keywords: Cu bonding; 3D packaging; Au nanolayer; Ag nanolayer; hybrid bonding



Citation: Lee, S.; Park, S.; Kim, S.E. Low-Temperature Diffusion of Au and Ag Nanolayers for Cu Bonding. *Appl. Sci.* **2024**, *14*, 147. <https://doi.org/10.3390/app14010147>

Academic Editor: Alex Fragoso

Received: 30 November 2023

Revised: 19 December 2023

Accepted: 20 December 2023

Published: 23 December 2023



Copyright: © 2023 by the authors. Licensee MDPI, Basel, Switzerland. This article is an open access article distributed under the terms and conditions of the Creative Commons Attribution (CC BY) license (<https://creativecommons.org/licenses/by/4.0/>).

1. Introduction

Semiconductor devices have shown improved performance and integration according to Moore's law, which states that the number of transistors that can be integrated doubles every 18 months. However, as technology advances, the need for multi-functional, high-performance, and high-capacity electronic devices is also increasing. Accordingly, the miniaturization of semiconductor devices, which were developed according to Moore's law, has also faced limitations. To overcome this, various semiconductor manufacturing process technologies are being developed, and in particular, technologies in the packaging stage, which are post-processes, are also being studied. Three-dimensional packaging technologies with higher density levels and performance capabilities than existing two-dimensional packaging technologies and that have the advantages of a smaller size and lower production cost are being studied continually. Three-dimensional packaging technology is characterized by vertically stacked semiconductor devices, including TSV (through silicon via), a technology that connects stacked chips to electrodes through fine, etched holes, wafer grinding, and bonding to stack various chips vertically [1]. There are different methods of bonding, such as the wafer-to-wafer (W2W), chip-to-wafer (C2W), and chip-to-chip (C2C) types. In general, the W2W stacking method is favored due to its compatibility with processing in a vacuum environment, thereby minimizing the risk of Cu surface oxidation and enhancing ultra-fine misalignment capabilities. On the other hand, the C2W or C2C stacking methods present challenges such as fine misalignment issues of less than half

a micron and Cu oxidation during dicing and chip transfer processes. In the context of device stacking, the arrangement methods can be divided into face-to-face bonding and face-to-back bonding.

There are many bonding methods for Cu bonding. The surface-activated bonding (SAB) method allows room temperature bonding by removing copper oxide on the surface using Ar plasma and subsequently activating the surface for bonding in ultra-high vacuum conditions. However, due to the demanding nature of ultra-high vacuum processes and the potential reliability degradation from the high-energy impact of Ar plasma, this method has not been widely adopted for mass production. Wet processes using chemical solutions such as acetic acid, sulfuric acid, and hydrochloric acid are also available as an alternative to plasma for copper oxide removal. However, treating completed components with acidic solutions is considered unsuitable for mass production due to the potential performance degradation. An alternative method for achieving low-temperature bonding while preventing copper surface oxidation involves the use of a self-assembled monolayer (SAM). This method entails coating the copper surface with a polymer-based SAM, adsorbing it to the copper surface, and then detaching it during bonding. Although SAMs can prevent copper oxidation, achieving complete detachment may require temperatures close to 250 °C. The presence of residual SAM on the copper surface or decomposed SAM remnants in the chamber may pose compatibility issues with semiconductor processes. Among various copper bonding methods, the most suitable for semiconductor CMOS devices' mass production and high-performance computing (HPC) applications in next-generation stacked packaging is metal/dielectric hybrid bonding. Metal/dielectric hybrid bonding is gaining increased attention, driven by the rising number of input/output bumps and a rapid reduction in bump pitch. As a metal, copper (Cu) has been used as a bonding material owing to its excellent electrical properties, thermal conductivity, and low cost [2]. As dielectric materials, SiCN, SiO₂, benzocyclobutene (BCB), and polyimide (PI) are commonly used. Since both Au and Ag can be employed in the CMP process, they can be applied in Cu/dielectric hybrid bonding as a metal passivation layer on the Cu surface.

The mechanism of metal-to-metal wafer bonding consists of diffusion of the metal at the bonding interface [3]. Accordingly, for smooth bonding, it is necessary to keep the metal as clean as possible. However, due to the characteristics of Cu, there is a disadvantage in that oxidation occurs very easily in air. Many studies are being conducted in an effort to prevent this [4–8]. For example, a two-step plasma treatment using Ar and N₂ was applied to the Cu surface to remove Cu oxide and to activate the Cu surface so as to form a nanometer-level Cu nitride (Cu₄N) layer to serve as a bonding interface [4]. Other researchers attempted to prevent Cu oxidation and to realize pure Cu-to-Cu bonding by depositing nanometer-level metal thin-film passivation layers consisting of, for instance, titanium (Ti), silver (Ag), and gold (Au), on the Cu surface [5–7]. Practically, to activate Cu diffusion at the bonding interface and also decompose natural Cu oxide films, Cu bonding lasting approximately one hour at a high temperature of at least 400 °C is necessary [8]. However, a bonding process at a high temperature can subject semiconductor devices to excessive thermal and mechanical stress; thus, low-temperature Cu bonding studies are needed for three-dimensional stacked structures. Cu bonding using a <111> Cu nanotinned structure was reported at about 200 °C [9], and Cu bonding using a nanolayer of Au was reported at a temperature of 150 °C [10]. Also, Cu bonding using a nanolayer of Ag was reported at a temperature of 180 °C [11]. Both studies confirmed that Cu can be bonded at a temperature of less than 200 °C, demonstrating that the material deposited with a thin-film passivation layer and Cu were mutually diffused to form a bonded interface. The biggest advantage of the method using the metal passivation nanolayer is that only this method enables Cu bonding at a temperature lower than 200 °C [12]. However, since the two materials are mutually diffused after passivation metal is deposited on Cu, IMC (intermetallic compound) can be generated, which can cause problems with mechanical and electrical reliability [13].

In this study, Cu-to-Cu bonding was evaluated using Au and Ag nanolayers to prevent Cu oxidation on the Cu surface prior to bonding and to induce solid-state diffusion to form a uniform Cu bonding interface. Au is rarely oxidized, prevents Cu from being oxidized, has excellent electrical conductivity, has high chemical stability, and can be planarized by a chemical mechanical polishing (CMP) process [14]. Ag, like Au, has very good electrical conductivity and a damascene process using CMP is possible [15]. However, Ag can be oxidized and has a higher Young's modulus and coefficient of thermal expansion than Au. The material properties of Au and Ag are listed in Table 1. As mentioned above, the objective of employing metal passivation in Cu bonding is to achieve a robust Cu bond at temperatures below 200 °C, as Cu is not significantly thermally expanded at this range, ensuring a secure bond. So, in this study, bonding experiments were conducted at 180 °C, and the characteristics between the Au and Ag passivation layers were compared. In addition, the diffusion properties of each material were investigated at various temperatures. Other studies [3,10–12,16,17] have already reported low-temperature Cu bonding using Au or Ag, but this study aims to investigate diffusion characteristics of evaporated Au and Ag into Cu and identify mechanisms between them.

Table 1. Material properties of Au, Ag, and Cu.

Element	Au	Ag	Cu
Atomic Number	79	47	29
Empirical Radius (pm)	144	144	128
Young's Modulus (GPa)	79	83	110~128
Poisson's Ratio	0.4	0.37	0.34
Electrical Resistivity (nΩ·m at 20 °C)	22.14	15.87	16.78
Density (g/cm ³)	19.3	10.49	8.96
CTE (mm/(m·K) at 25 °C)	14.2	18.9	16.5
Melting Point (°C)	1067.18	961.78	1084.62
Crystal Structure	FCC	FCC	FCC
Electronegativity	2.54	1.93	1.90

2. Materials and Methods

In this study, an e-beam evaporator (Evaporation System, SRN-200, Sorona Inc., San Luis Obispo, CA, USA) was used to deposit the Au and Ag, and sputter (Sputtering system, SRN-110, Sorona Inc.) was used to deposit Ti layer followed by Cu layer. Evaporated Au and Ag nanolayers tend to form porous films rather than thin films, which is expected to facilitate solid diffusion with the Cu thin film layer. An 8-inch silicon wafer (100) was thermally oxidized (Diffusion Furnace, SJF-1000, DS GLOBAL, Seoul, Republic of Korea) to grow approximately 0.7 μm of SiO₂ and then diced (Automatic Dicing Saw DAD 3350, DISCO Corporation, Tokyo, Japan) to 1 cm × 1 cm. After the dicing step, Au or Ag nanolayers were deposited on the Cu surface to a thickness of approximately 12~15 nm. During our evaporation process, the deposition rate was so fast that it was very difficult to control the thickness to less than 10 nm. For this reason, we have deposited 12 nm Au and 15 nm Ag nanolayers on the Cu surface.

To confirm how Au and Ag mutually diffuse with Cu, an XPS (X-ray photoelectron spectroscopy, Thermo Fisher Scientific Brno s.r.o, Nexsa, Brno, Czech Republic) analysis was utilized. The specimens were processed as follows: Ti was sputtered with a thickness of 50 nm as an adhesion layer on the Si/SiO₂ surface, after which 1 μm of Cu film was sputtered. Afterwards, 12 nm of Au or 15 nm of Ag was deposited by e-beam evaporator, and the specimens were heated on a hot plate at temperatures of 25 °C, 100 °C, 150 °C, and 200 °C for one hour to evaluate the degree of mutual diffusion. The process flow for the diffusion test is presented in Figure 1. The film structure was analyzed by TEM

(transmission electron microscope, JEM-3010, Oxford X-Max 80T, Abingdon-on-Thames, UK) measurements in addition to the XPS measurements.

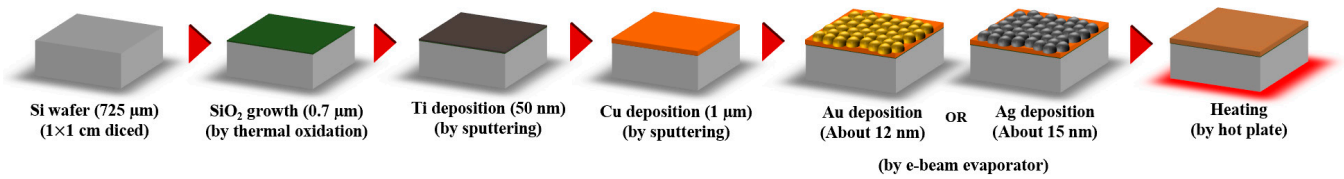


Figure 1. Schematic diagram of heating test process to investigate the diffusion between passivation metal and Cu.

Finally, Cu bonding was performed using Au or Ag as a passivation layer. In this study, W2W bonding (SB 8e, Suss Microtec, Garching, Germany) was employed. The process flow for the bonding is presented in Figure 2. As shown in Figure 2, the top wafer was fabricated with 1 cm \times 1 cm square Cu structures and bonded to the bottom wafer on a Cu blanket film. The bonding procedure was conducted at 180 $^{\circ}\text{C}$ under a pressure of 0.8 MPa for 30 min. Subsequently, an annealing step was performed at 200 $^{\circ}\text{C}$ under a pressure of 0.2 MPa for a duration of 60 min. Both the bonding temperature and annealing temperature were chosen to achieve Cu bonding at temperatures below 200 $^{\circ}\text{C}$, facilitating low-temperature Cu bonding with the use of a metal passivation layer. The temperature was ramped up from room temperature to 180 $^{\circ}\text{C}$ at first, and then bonding and annealing processes were performed. Inside the bonding chamber, a base pressure of 5×10^{-5} mbar was maintained from the beginning to the end of the process. The effects of the annealing process are reported in the literature [18]. To analyze the quality of the bonding interface after the bonding process, a SAT (scanning acoustic tomography, FS 200 III, Hitachi, Tokyo, Japan) analysis was conducted, after which FE-SEM (field emission-scanning electron microscope, High Technologies Corporation (SU8010), Hitachi, Tokyo, Japan) and Cs-STEM (spherical aberration corrector scanning transmission electron microscope, NEO ARM, JEOL, Tokyo, Japan) measurements were taken. The shear strength of the bonded specimen was measured using a shear strength tester (Bondtester, Dage 4000 Plus, Dako Co., Ltd., Seoul, Republic of Korea).

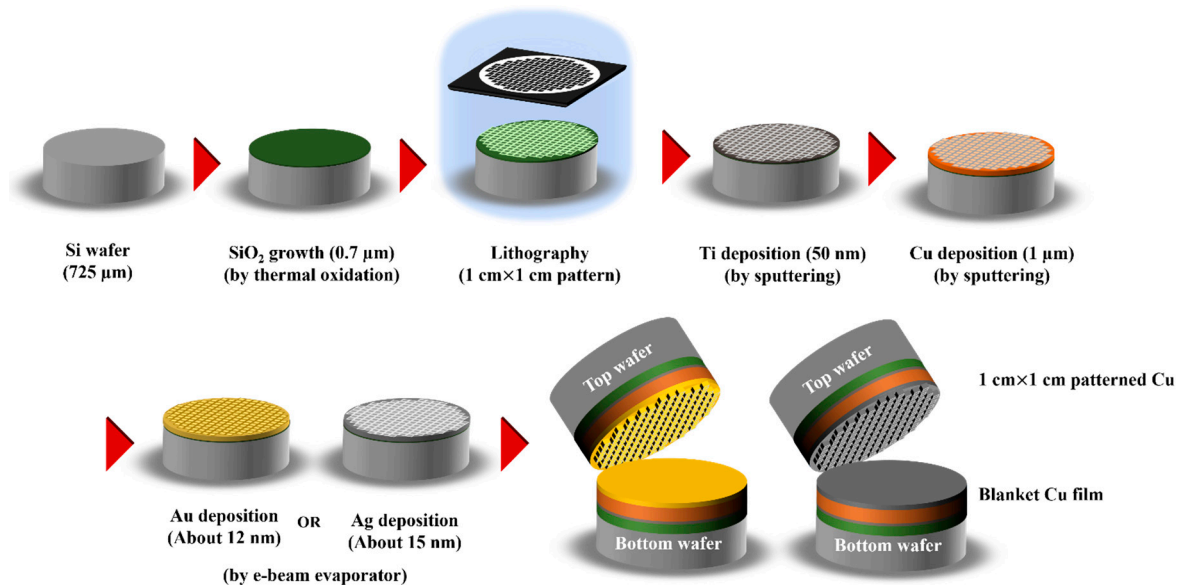


Figure 2. Schematic diagram of the bonding specimens in this study.

3. Results and Discussion

An SEM analysis was conducted to observe the state of the Au and Ag layers deposited by e-beam evaporation. As shown in Figure 3, Au and Ag similarly exhibited porous structures and non-film-like layers, characteristic of metal deposited using an e-beam evaporator. Given that the materials were deposited in a porous form, the deposition thickness was not perfectly uniform. Here, the Au and Ag layers were deposited at average thicknesses of about 12 nm and 15 nm, respectively.

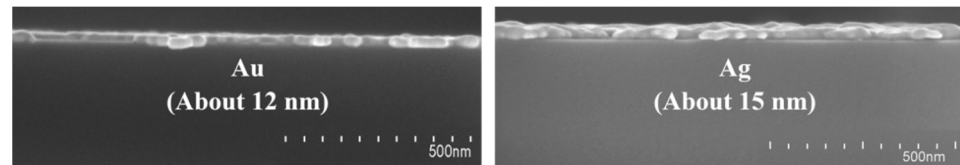


Figure 3. SEM image of Au and Ag deposited using an e-beam evaporator.

The chemical state and amount of each element (Au, Ag, Cu, and O) were determined by XPS, as shown in Figure 4, to discern the diffusion characteristics between Ag and Cu, and between Au and Cu. First, for Au and Cu, it was found that the atomic percentage of Au gradually decreases on the surface and the atomic percentage of Cu gradually increases as the temperature increases. In addition, O increases as Cu increases on the surface, likely a phenomenon caused by oxidation due to the increased Cu on the surface as Cu diffuses more actively to Au at higher temperatures. At 25 °C, there is a very small amount of O at the surface compared to the Ag-Cu case. For Ag and Cu, as the temperature increases, the atomic percentage of Ag on the surface gradually decreases, with Ag completely diffused into Cu at 200 °C. The Au and the Ag surfaces both have oxygen because they both have porous structures; in particular, Ag tends to be easily oxidized compared to Au. In Figure 4e, The O1s peak profile shows that CuO becomes more prominent than Cu₂O as the temperature increases, as Cu is more oxidized and forms a more stable state from Cu₂O to CuO [19]. Also, under high-temperature heating, the chemisorbed OH- peak appeared to be distinctly high. On the other hand, for Ag, it was observed that Cu₂O changes to CuO as the temperature increases, but unlike the Au case, there is almost no chemisorbed OH- peak, and a strong satellite peak appears around 942 eV, as shown in Figure 4d. The presence of this satellite peak indicates a similar coexistence of Cu²⁺ and Cu⁺, although Cu²⁺ may be more abundant [20]. As shown in Figure 4e,f, oxygen content was observed on the surface before the bonding process in this study due to a porous form of metal nanolayer. To control oxygen permittivity on the bonding surface, a more densely structured metal layer may be required, especially given the use of a nanolayer.

Next, the diffusion activation energy required for diffusion between Au and Cu, Ag, and Cu was estimated using the data obtained through the XPS analysis and with the Arrhenius equation below. In Equation (1) below, K is the amount of each element obtained through the XPS analysis, A is the diffusion constant, E_a is the diffusion activation energy, R is the gas constant (8.314 J·K⁻¹·mol⁻¹), and T is the absolute temperature value.

$$K = A \exp\left(\frac{-E_a}{RT}\right) \quad (1)$$

If natural logarithms are taken on both sides of the above equation, it can be transformed in the following way.

$$\ln(K) = \ln(A) - \left(\frac{E_a}{R}\right) \left(\frac{1}{T}\right) \quad (2)$$

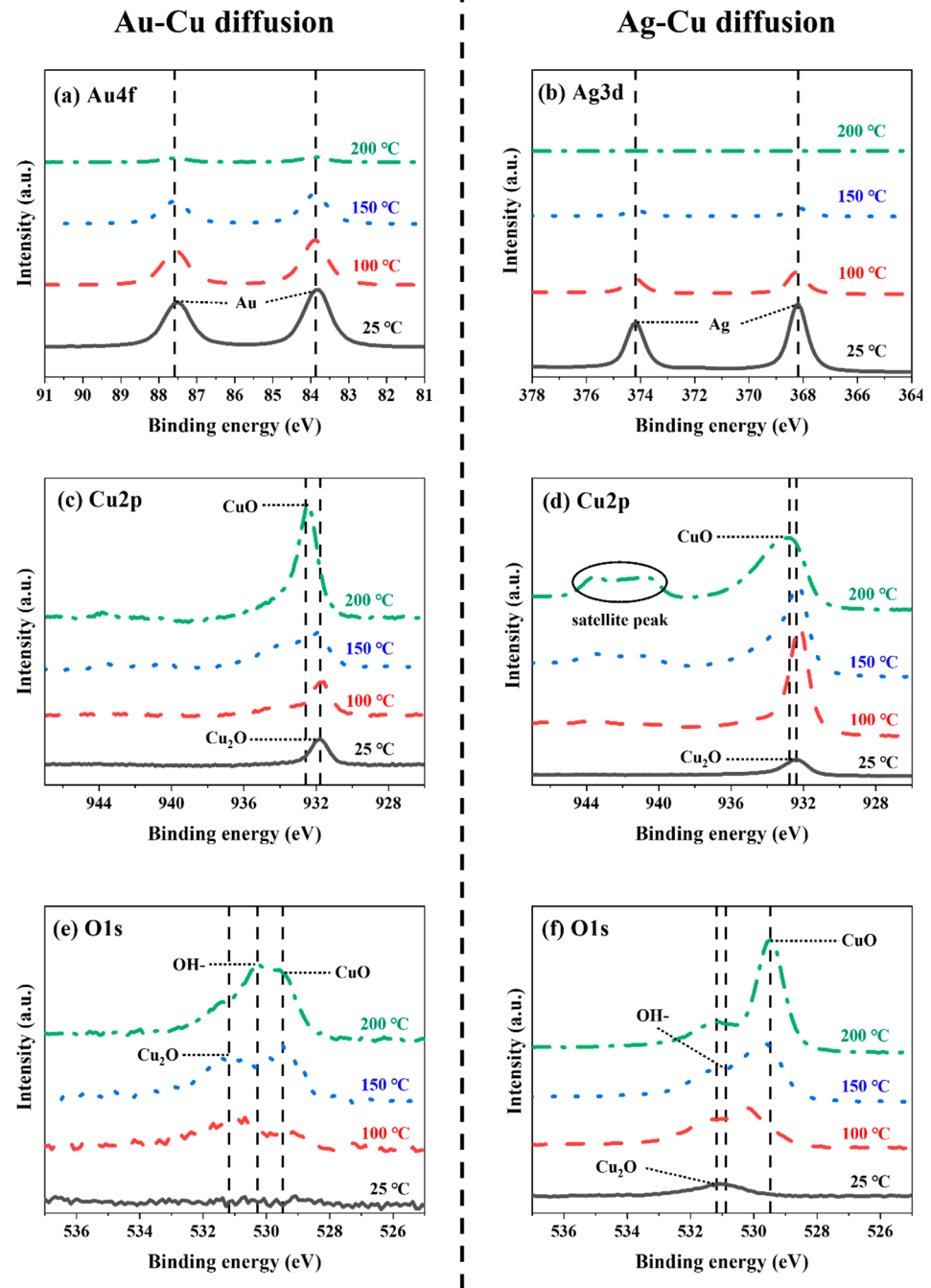


Figure 4. Evaluation of surface XPS peak profiles: (a) Au4f peak profile in Au-Cu diffusion, (b) Ag3d peak profile in Ag-Cu diffusion, (c) Cu2p peak profile in Au-Cu diffusion, (d) Cu2p peak profile in Ag-Cu diffusion, (e) O1s peak profile in Au-Cu diffusion, (f) O1s peak profile in Ag-Cu diffusion.

The diffusion activation energy obtained through Equation (2) for Au and Cu was 6369.52 J/mol when Au diffuses to Cu, and 9816.50 J/mol when Cu diffuses to Au, as shown correspondingly in Figure 5a,b. The lower the diffusion activation energy, the easier the diffusion; hence, according to this result, it is believed that the diffusion of Cu into Au was more difficult than the diffusion of Au into Cu. As shown in Figure 5c,d, the diffusion activation energy for Ag and Cu was 17,933.21 J/mol when Ag diffuses into Cu and 15,626.82 J/mol when Cu diffuses into Ag, unlike the Au case, showing that the diffusion of Cu into Ag is easier than the diffusion of Ag into Cu. Ag has similar electronegativity toward Cu, while Au has stronger electronegativity toward Cu. Additionally, Ag may be

oxidized at the surface, whereas Au does not oxidize at all. Therefore, diffusion from Cu to Ag requires less energy than diffusion from Ag to Cu, while diffusion from Cu to Au requires greater activation energy than diffusion from Au to Cu.

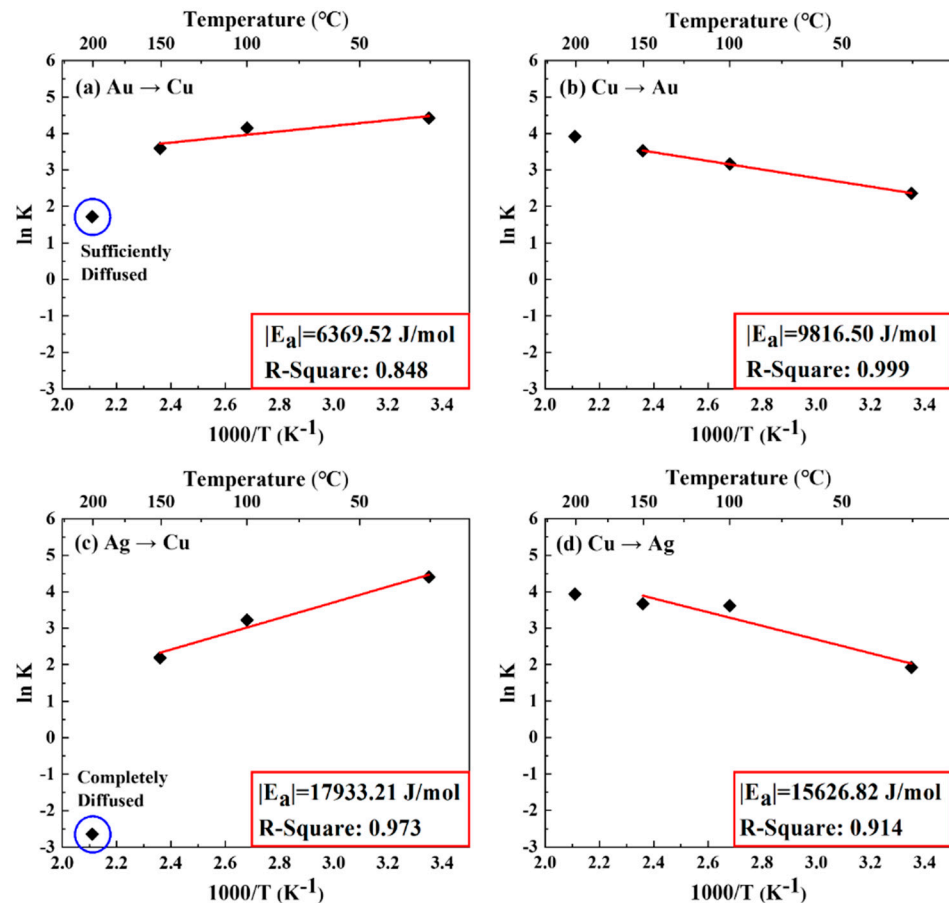


Figure 5. Estimation of diffusion activation energy between Au-Cu and Ag-Cu layers: (a) diffusion from Au to Cu diffusion, (b) diffusion from Cu to Au, (c) diffusion from Ag to Cu, (d) diffusion from Cu to Ag.

Based on the phase diagrams of Au-Cu [21] and Ag-Cu [22], AuCu₃ may exist at 200 °C if an alloy is formed between Au and Cu, but Figure 4a,c show no evidence of the formation of the AuCu₃ alloy. For Ag-Cu, mostly the α phase, which is the Cu phase, may exist at 200 °C with a minuscule amount of the α phase. In this study, IMC (intermetallic compound) formation was not observed for either Au or Ag due to non-bulk diffusion at high temperatures. The diffusion activation energy value estimated in this study was compared with the diffusion activation energy value of Au and Cu at bulk levels at high temperatures. The activation energy of Au-Cu bulk diffusion at above 700 °C was approximately 178~197 kJ/mol when Au diffuses to Cu and about 169~172 kJ/mol when Cu diffuses to Au [23,24]. In addition, the activation energy of Ag-Cu bulk diffusion at temperatures exceeding 700 °C was about 184~198 kJ/mol when Ag diffuses to Cu and about 192 kJ/mol when Cu diffuses to Ag [23,24]. Given that diffusion at low temperatures primarily occurs in the form of grain boundary diffusion rather than lattice diffusion, it is unsurprising that the diffusion activation energy observed in this study is lower compared to diffusion at elevated temperatures. Within the scope of this study, distinct diffusion behaviors of Cu on the surface were observed when comparing porous Au and Ag nanolayers with bulk Cu films. In the context of Au-Cu interactions, it was evident that Au exhibited rapid diffusion into Cu, whereas in the Ag-Cu scenario, Cu demonstrated rapid diffusion into Ag.

In general, a high temperature of over 400 °C is required to facilitate Cu bonding, though this can deteriorate the performance of semiconductor devices [25]. In addition, the bonding temperature of semiconductors varies depending on the product, but low temperatures below 250 °C are increasingly required. Cu bonding using a metal passivation layer can be applied to products either ultra-fine pitch Cu pad structures or larger Cu pad structures with a low Cu volume that does not sufficiently expand at low bonding temperatures. In this study, Cu bonding was evaluated at a temperature of 180 °C, and annealing was carried out at a temperature of 200 °C. Figure 6 shows the ion beam milling preprocessing conducted for SEM and TEM measurements of the bonding interface. Figure 7 shows the SAT images of the Cu bonding interface with Au and Ag nanolayers. Figure 8 shows the FE-SEM and TEM results of the Cu bonding interface using an Au nanolayer. In the FE-SEM image shown in Figure 8a,b, the black area is Cu and oxygen introduced before bonding, and the white line next to the black area is Au. According to the EDS (energy dispersive spectroscopy) line mapping chart in Figure 8c, a large amount of oxygen was observed at the interface. It is believed that oxygen contamination was already present at the Au and Cu interface before bonding. Figure 9 shows the FE-SEM and TEM results of the Cu bonding interface using an Ag nanolayer. The use of the Ag nanolayer also led to a pattern very similar to that of the Au nanolayer. However, in contrast to when the Au nanolayer was used, for the Ag nanolayer, oxygen is not observed solely at the Cu region of the interface; instead, it seems to be widely dispersed throughout the bonding interface. This suggests an oxidation process occurring in the Ag nanolayer. Despite the presence of oxygen inflow prior to bonding, it was verified that oxidation of the Ag nanolayer occurred. There is a strong probability that both Ag and AgO diffusion took place during the Ag-Cu interaction. When evaporated Au and Ag diffused inward during the bonding and annealing process, the interface was filled with Cu and O at the surface before bonding.

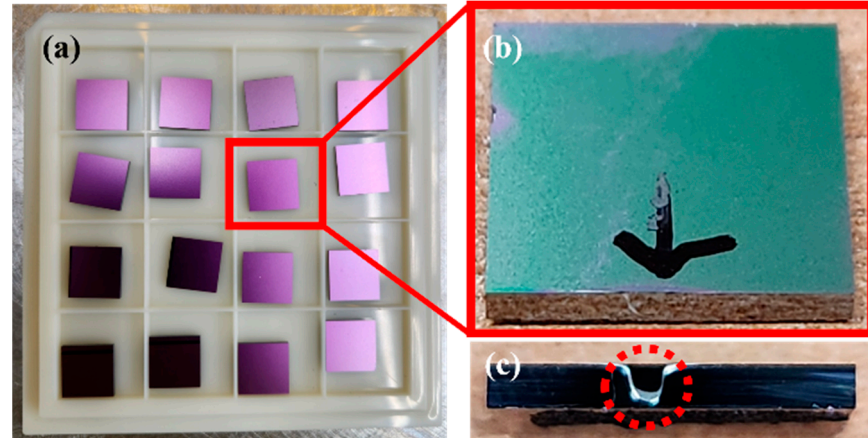


Figure 6. Sample preparation for TEM. (a) diced chips after bonding; (b) tilt view of one diced chip; (c) chip pretreated by ion beam milling.

The bonding strength of the bonded specimen was evaluated by shear strength measurements. A specimen of 2 mm × 2 mm in size was used, and the average value was calculated from 20 shear strength measurements. The bottom part of the diced chip was fixed with a zig, and the tip was moved at a speed of 600 μm/s to measure the shear strength when separated by pushing the top part. As shown in Figure 10, the average shear strength of Cu bonding using an Au and an Ag nanolayer was 5.39 MPa and 6.55 MPa, respectively. For Cu bonding using the Au nanolayers, the average value was slightly lower, and the standard deviation was slightly broader than that of Cu bonding using Ag nanolayers. The relatively low shear strength values in this study can be attributed to two factors: firstly, the low bonding pressure utilized, and secondly, the presence of the non-uniform presence of a metal layer at the bonding interface. To enhance the shear strength of the bonding interface, it is essential to explore a thinner metal passivation layer.

Also, the annealing process significantly contributes to improving bonding strength and Cu diffusion. Our current annealing temperature is set at 200 °C, which is the maximum temperature intended for the low-temperature Cu bonding system. Therefore, we may explore the possibility of extending the annealing temperature for further optimization.

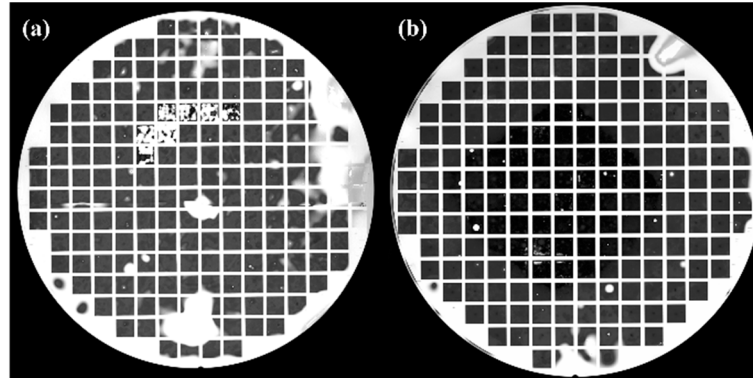


Figure 7. SAT image of a bonded wafer. (a) Au; (b) Ag [16] nanolayer.

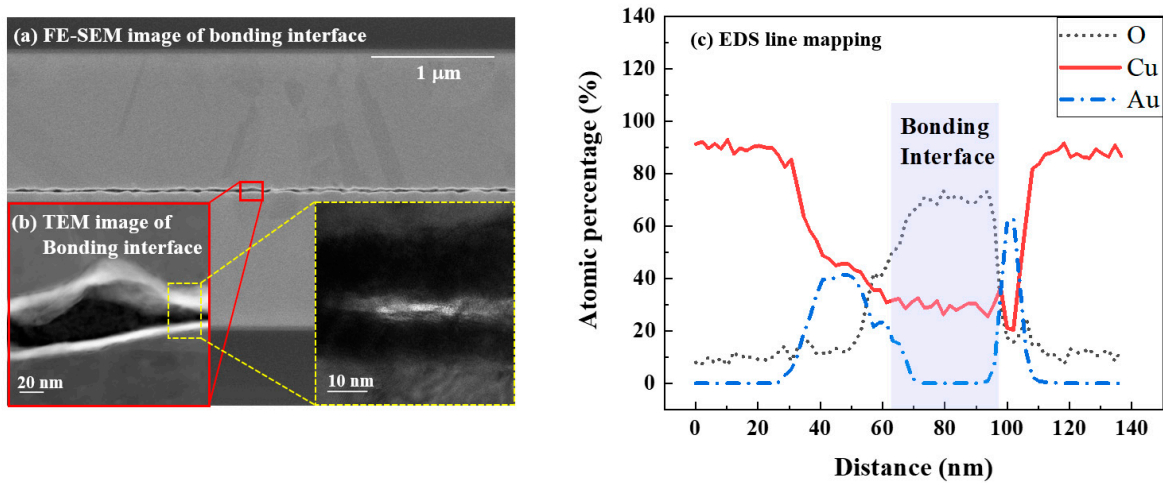


Figure 8. (a) FE-SEM and (b) TEM analysis results of a bonded wafer using an Au passivation nanolayer and (c) EDS scanning results.

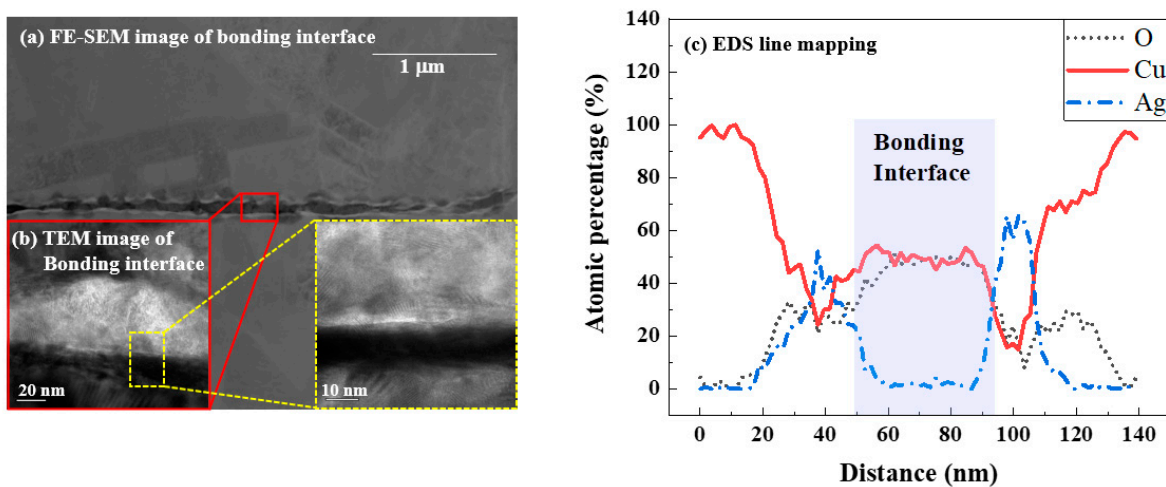


Figure 9. (a) FE-SEM and (b) TEM analysis results of a bonded wafer using an Ag passivation nanolayer and (c) EDS scanning results.

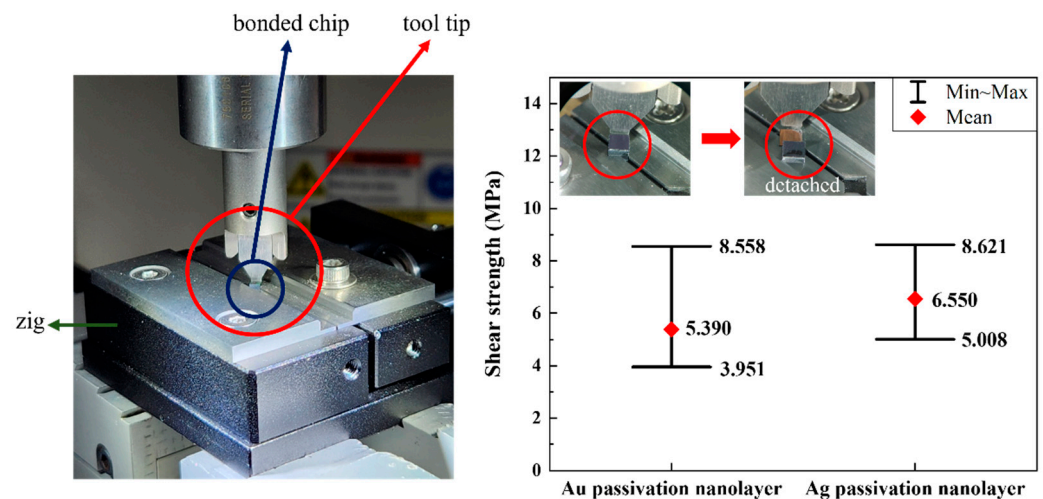


Figure 10. Shear test results when using Au and Ag nanolayers with Cu bonding: (left) shear testing jig and tool tip and (right) bonding strength measured by shear testing.

4. Conclusions

In this study, we conducted a comparative analysis of Au and Ag nanolayers as passivation layers to facilitate low-temperature Cu-Cu bonding for hybrid bonding applications. Au and Ag nanolayers were deposited using an e-beam evaporator, and Cu-Cu bonding was conducted at a low temperature of 180 °C. The diffusion behavior of Cu film exhibited distinct characteristics when interacting with porous Au and Ag nanolayers. For Au-Cu interaction, the activation energy for the diffusion of Au into Cu was found to be lower than that of Cu into Au. Conversely, for Ag-Cu interaction, the activation energy for the diffusion of Ag into Cu was found to be higher than that of Cu into Ag. When comparing the behaviors of the Au and Ag nanolayers, Cu exhibited more pronounced diffusion towards the bonding interface when an Ag nanolayer was employed. Cu bonding using a metal passivation layer can be applied to both ultra-fine pitch Cu pad structures and larger Cu pad structures with a low Cu volume that does not sufficiently expand at low bonding temperatures.

Author Contributions: Conceptualization, S.E.K.; formal analysis, S.L.; funding acquisition, S.E.K.; investigation, S.L. and S.P.; methodology, S.L.; supervision, S.E.K.; validation, S.L., S.P. and S.E.K.; visualization, S.L.; writing—original draft, S.L.; writing—review and editing, S.E.K. All authors have read and agreed to the published version of the manuscript.

Funding: This research was supported by the National R&D Program through the National Research Foundation of Korea (NRF) funded by the Ministry of Science and ICT (No. 2022M3I7A4072293) and was partially supported by the Technology Innovation Program (public-private joint investment semiconductor R&D program (K-CHIPS) to foster high-quality human resources) (RS-2023-00236091, hybrid bonding technologies for 3D package interconnects) funded by the Ministry of Trade, Industry and Energy (MOTIE, Republic of Korea) (1415187584).

Institutional Review Board Statement: Not applicable.

Informed Consent Statement: Not applicable.

Data Availability Statement: All data analyzed during this study are included in this published article.

Conflicts of Interest: The authors declare no conflict of interest.

References

- Shen, W.W.; Chen, K.N. Three-dimensional integrated circuit (3D IC) key technology: Through-silicon via (TSV). *Nanoscale Res.* **2017**, *12*, 56. [[CrossRef](#)] [[PubMed](#)]
- Li, J.; Yu, X.; Shi, T.; Cheng, C.; Fan, J.; Cheng, S.; Liao, G.; Tang, Z. Low-temperature and low-pressure Cu-Cu bonding by highly sinterable Cu nanoparticle paste. *Nanoscale Res. Lett.* **2017**, *12*, 255. [[CrossRef](#)] [[PubMed](#)]

3. Bonam, S.; Panigrahi, A.K.; Kumar, C.H.; Vanjari, S.R.K.; Singh, S.G. Interface and reliability analysis of Au-passivated Cu-Cu fine-pitch thermocompression bonding for 3-D IC applications. *IEEE Trans. Compon. Packag. Manuf. Technol.* **2019**, *9*, 1227–1234. [[CrossRef](#)]
4. Park, H.; Seo, H.; Kim, Y.; Park, S.; Kim, S.E. Low-temperature (260 °C) solderless Cu-Cu bonding for fine-pitch 3-D packaging and heterogeneous integration. *IEEE Trans. Compon. Packag. Manuf. Technol.* **2021**, *11*, 565–572. [[CrossRef](#)]
5. Huang, Y.P.; Chien, Y.S.; Tzeng, R.N.; Shy, M.S.; Lin, T.H.; Chen, K.H.; Chiu, C.T.; Chiou, J.C.; Chuang, C.T.; Hwang, W.; et al. Novel Cu-to-Cu bonding with Ti passivation at 180 °C in 3-D integration. *IEEE Electron Dev. Lett.* **2013**, *34*, 1551–1553. [[CrossRef](#)]
6. Kim, Y.; Park, S.; Kim, S.E. The effect of an Ag nanofilm on low-temperature Cu/Ag-Ag/Cu chip bonding in air. *Appl. Sci.* **2021**, *11*, 9444. [[CrossRef](#)]
7. Liu, D.; Chen, P.C.; Chou, T.C.; Hu, H.W.; Chen, K.N. Demonstration of low-temperature fine-pitch Cu/SiO₂ hybrid bonding by Au passivation. *IEEE J. Electron Devices Soc.* **2021**, *9*, 868–875. [[CrossRef](#)]
8. Park, H.; Seo, H.; Kim, S.E. Antioxidant copper layer by remote-mode N₂ plasma for low-temperature copper-copper bonding. *Sci. Rep.* **2020**, *10*, 21720. [[CrossRef](#)]
9. Chiu, W.L.; Lee, O.H.; Chiang, C.W.; Chang, H.H. Low temperature wafer-to-wafer hybrid bonding by nanotwinned copper. In Proceedings of the 2021 IEEE 71st Electronic Components and Technology Conference (ECTC), San Diego, CA, USA, 1 June–4 July 2021; pp. 365–370.
10. Liu, D.; Chen, P.C.; Tsai, Y.C.; Chen, K.N. Low-temperature Cu-to-Cu direct bonding below 150 °C with Au passivation layer. In Proceedings of the 2019 International 3D Systems Integration Conference (3DIC), Sendai, Japan, 8–10 October 2019; pp. 1–4.
11. Chou, T.C.; Huang, S.Y.; Chen, P.J.; Hu, H.W.; Liu, D.; Chang, C.W.; Ni, T.H.; Chen, C.J.; Lin, Y.M.; Chang, T.C.; et al. Electrical and reliability investigation of Cu-to-Cu bonding with a silver passivation layer in 3-D integration. *IEEE Trans. Compon. Packag. Manuf. Technol.* **2021**, *11*, 36–42. [[CrossRef](#)]
12. Hong, Z.J.; Liu, D.; Hu, H.W.; Cho, C.I.; Weng, M.W.; Liu, J.H.; Chen, K.N. Investigation of bonding mechanism for low-temperature Cu-Cu bonding with passivation layer. *Appl. Surf. Sci.* **2022**, *592*, 153243. [[CrossRef](#)]
13. Carro, L.D.; Zürcher, J.; Drechsler, U.; Clark, I.E.; Ramos, G.; Brunschwiler, T. Low-temperature dip-based all-copper interconnects formed by pressure-assisted sintering of copper nanoparticles. *IEEE Trans. Compon. Packag. Manuf. Technol.* **2019**, *9*, 1613–1622. [[CrossRef](#)]
14. Karbasian, G.; Fay, P.J.; Xing, H.G.; Orlov, A.O.; Snider, G.L. Chemical mechanical planarization of gold. *J. Vac. Sci. Technol.* **2014**, *32*, 021402. [[CrossRef](#)]
15. Emlinga, R.; Schindler, G.; Steinlesberger, G.; Engelhardt, M.; Gao, L.; Landsiedel, D.S. Deposition and CMP of sub 100 nm silver damascene lines. *Microelectron. Eng.* **2005**, *82*, 273–276. [[CrossRef](#)]
16. Kim, Y.; Kim, S.E. Effect of the annealing process on Cu bonding quality using Ag nanolayer. *IEEE Trans. Compon. Packag. Manuf. Technol.* **2023**, *13*, 737–742. [[CrossRef](#)]
17. Liu, Z.; Cai, J.; Wang, Q.; Wang, Z.; Liu, L.; Zou, G. Thermal-stable void-free interface morphology and bonding mechanism of low-temperature Cu-Cu bonding using Ag nanostructure as intermediate. *J. Alloys Compd.* **2018**, *767*, 575–582. [[CrossRef](#)]
18. Chua, S.L.; Chan, J.M.; Goh, S.C.K.; Tan, C.S. Cu–Cu bonding in an ambient environment by Ar/N₂ plasma surface activation and its characterization. *IEEE Trans. Compon. Packag. Manuf. Technol.* **2019**, *9*, 596–605. [[CrossRef](#)]
19. Sabat, K.C.; Paramguru, R.K.; Mishra, B.K. Reduction of copper oxide by low-temperature hydrogen plasma. *Plasma Chem. Plasma Process.* **2016**, *36*, 1111–1124. [[CrossRef](#)]
20. Biesinger, M.C.; Hart, B.R.; Polack, R.; Kobe, B.A.; Smart, R.S.C. Analysis of mineral surface chemistry in flotation separation using imaging XPS. *Miner. Eng.* **2007**, *20*, 152–162. [[CrossRef](#)]
21. Singh, A.; Pradeepkumar, M.S.; Jarwal, D.K.; Jit, S.; Bysakh, S.; Ahmad, M.I.; Basu, J.; Mandal, R.K. Homogeneous and polymorphic transformations to ordered intermetallics in nanostructured Au–Cu multilayer thin films. *J. Mater. Sci.* **2021**, *56*, 16113–16133. [[CrossRef](#)]
22. Kawecki, A.; Knych, T.; Smaga, E.S.; Mamala, A.; Kwasniewski, P.; Kiesiewicz, G.; Smyrak, B.; Pacewicz, A. Fabrication, properties and microstructures of high-strength and high-conductivity copper-silver wires. *Arch. Metall. Mater.* **2012**, *57*, 1261–1270. [[CrossRef](#)]
23. Brandes, E.A.; Brook, G.B. *Smithells Metals Reference Book*, 7th ed.; Butterworth-Heinemann: Oxford, UK, 1998.
24. Butrymowicz, D.B.; Manning, J.R.; Read, M.E. Diffusion in copper and copper alloys, part II. Copper-silver and copper-gold systems. *J. Phys. Chem. Ref. Data* **1974**, *3*, 527–602. [[CrossRef](#)]
25. Tang, Y.S.; Chang, Y.J.; Chen, K.N. Wafer-level Cu-Cu bonding technology. *Microelectron. Reliab.* **2012**, *52*, 312–320. [[CrossRef](#)]

Disclaimer/Publisher’s Note: The statements, opinions and data contained in all publications are solely those of the individual author(s) and contributor(s) and not of MDPI and/or the editor(s). MDPI and/or the editor(s) disclaim responsibility for any injury to people or property resulting from any ideas, methods, instructions or products referred to in the content.